Anisotropy of magnetic susceptibility in alkali feldspar and plagioclase

Andrea R. Biedermann,[1,*] Thomas Pettke,[2] Ross J. Angel[3] and Ann M. Hirt[1]

[1]*Institute of Geophysics, ETH Zurich, Sonneggstrasse 5, CH-8092 Zurich, Switzerland. E-mail: ann.hirt@erdw.ethz.ch*
[2]*Institute of Geological Sciences, University of Bern, Baltzerstrasse 1–3, CH-3012 Bern, Switzerland*
[3]*Department of Geosciences, University of Padova, Via G. Gradenigo 6, I-35134 Padova, Italy*

SUMMARY

Feldspars are the most abundant rock-forming minerals in the Earth's crust, but their magnetic properties have not been rigorously studied. This work focuses on the intrinsic magnetic anisotropy of 31 feldspar samples with various chemical compositions. Because feldspar is often twinned or shows exsolution textures, measurements were performed on twinned and exsolved samples as well as single crystals. The anisotropy is controlled by the diamagnetic susceptibility and displays a consistent orientation of principal susceptibility axes; the most negative or minimum susceptibility is parallel to [010], and the maximum (least negative) is close to the crystallographic [001] axis. However, the magnetic anisotropy is weak when compared to other rock-forming minerals, 1.53×10^{-9} m^3 kg^{-1} at maximum. Therefore, lower abundance minerals, such as augite, hornblende or biotite, often dominate the bulk paramagnetic anisotropy of a rock. Ferromagnetic anisotropy is not significant in most samples. In the few samples that do show ferromagnetic anisotropy, the principal susceptibility directions of the ferromagnetic subfabric do not display a systematic orientation with respect to the feldspar lattice. These results suggest that palaeointensity estimates of the geomagnetic field made on single crystals of feldspar will not be affected by a systematic orientation of the ferromagnetic inclusions within the feldspar lattice.

Key words: Magnetic and electrical properties; Magnetic fabrics and anisotropy; Palaeointensity; Rock and mineral magnetism.

1 INTRODUCTION

Feldspars are the most abundant constituent minerals in Earth's crust. They occur in igneous rocks covering basic to acidic and alkaline compositions, and as an accessory mineral in shallow ultrabasic rocks; they are often also important in metamorphic rocks. Feldspar is a Na–K–Ca–Al tectosilicate, generally poor in iron or other elements with strong magnetic moments (Deer *et al.* 2001). While both alkali feldspar and plagioclase have low susceptibilities, their abundance makes it important to characterize their magnetic properties, including their intrinsic magnetic anisotropy as well as the anisotropy arising from exsolution textures or inclusions within the crystals. Plagioclase, much more often than alkali feldspar, can contain small inclusions of ferromagnetic minerals. These ferromagnetic inclusions have been used in several early palaeomagnetic studies as palaeofield recorders (Evans & McElhinny 1966; Strangway *et al.* 1968; Murthy *et al.* 1971; Evans & Wayman

1974; Wu *et al.* 1974). Ferromagnetic inclusions within feldspar are preferred palaeomagnetic recorders, first because they are protected against alteration by the feldspar host (Cottrell & Tarduno 1999, 2000; Feinberg *et al.* 2005; Tarduno *et al.* 2006). Secondly, whereas magnetite forms large multidomain grains in pyroxenes or amphiboles, the inclusions in plagioclase are generally in the single-domain range and thus possess a stable remanence (Hargraves & Young 1969; Murthy *et al.* 1971). Finally, microtexture, for example, intraoxide exsolution, further strengthens the magnetic remanence of inclusions in plagioclase (Feinberg *et al.* 2005).

It has long been recognized that anisotropy can deviate the direction of remanent magnetization (Fuller 1960, 1963; Uyeda *et al.* 1963; Coe 1979). Concerns have therefore been raised, that the palaeointensity recorded by such grains can be affected by their preferred orientation, which in turn gives rise to magnetic anisotropy (Cottrell & Tarduno 1999; Selkin *et al.* 2000; Tarduno *et al.* 2006). Magnetite rods in plagioclase may form by exsolution of Fe^{2+} and Fe^{3+} that had been incorporated into the feldspar structure at high temperature. According to Davis (1981), magnetite exsolves along one or several of four directions of the plagioclase lattice. Wenk *et al.* (2011) observed that the long axes of magnetite needles are aligned with the plagioclase *c*-axis. Shape-preferred orientation of the

*Now at: Department of Geology and Mineral Resources Engineering, Norwegian University of Science and Technology, Sem Sælands vei 1, 7491 Trondheim, Norway.

magnetite will influence both the anisotropy of magnetic susceptibility (AMS) and the direction of the remanent magnetization, and consequently, the recorded palaeofield direction in individual feldspar crystals, or in rocks that contain feldspar with lattice-preferred orientation.

Given the abundance of feldspar and the supposedly high reliability of its ferromagnetic inclusions as palaeomagnetic recorders, it is surprising how little is known about the magnetic properties of single feldspar crystals. Only one measurement on magnetic anisotropy of an adularia crystal has been performed to date (Finke 1909). This study showed that the most negative principal susceptibility of diamagnetic adularia is tilted $-13°20'$ relative to the crystallographic [001] axis. The magnitudes of the maximum, intermediate and minimum susceptibilities were -5.47×10^{-9} m^3 kg^{-1}, -4.63×10^{-9} m^3 kg^{-1} and -4.09×10^{-9} m^3 kg^{-1}, respectively. Selkin *et al.* (2014) characterized magnetic anisotropy and its relation to mineral fabric in the Stillwater Complex. In plagioclase, they observed an oblate magnetic anisotropy with several orientations; for example, minimum susceptibility close to the crystallographic [001] direction of plagioclase and the maximum in the (001) plane, or close to the (100) direction. This anisotropy was interpreted to arise from elongated magnetite inclusions in feldspar. Selkin *et al.* (2000) investigated the influence of magnetic anisotropy on palaeointensity estimates in an anorthosite from the Stillwater Complex. They found that anisotropy of remanence can cause large variations in palaeointensity estimates and observed that the minimum principal susceptibility is normal to the plagioclase foliation and the maximum principal susceptibility aligns with the poorly defined grouping of plagioclase [001] axes. The observed anisotropy could arise from (1) the plagioclase itself or (2) inclusions within the plagioclase. Feinberg *et al.* (2006) studied the Bushveld layered intrusion and found that the (010) planes of plagioclase are parallel to foliation. The same preferred orientation was observed by Seront *et al.* (1993) in a study on the Oklahoma anorthosite. It can be assumed that this is the case in other plagioclase-bearing rocks that show preferred mineral alignment, as the crystals are often tabular with their short direction normal to (010) (Deer *et al.* 1992, 2001).

In the absence of ferromagnetic minerals, magnetic anisotropy of feldspar can arise from two sources: diamagnetic and paramagnetic anisotropy. Diamagnetism is related to the orbital moment of the electrons and is a property of all materials. If a magnetic field is applied to a diamagnetic material, the motion of the electrons is affected such that a secondary magnetic field is created antiparallel to the applied field. This causes a magnetization opposite to the applied field, and therefore, diamagnetic materials are characterized by a negative susceptibility (O'Handley 2000). The magnitude of the diamagnetic susceptibility is related to the area within the electrons orbit. Therefore, diamagnetic anisotropy arises if the electron orbit is of different size when the field is applied in different directions. The most negative susceptibility is expected normal to the lattice plane in which the electron movement is facilitated (Pauling 1936, 1979a). This effect has been observed in organic molecules, carbonate minerals and graphite (Krishnan 1934; Pauling 1936, 1979; Banerjee 1939; Krishnan & Ganguli 1939; Wallace 1947; McClure 1956a, 1979b; Schmidt *et al.* 2006, 2007a). Paramagnetism occurs in ions with unpaired electrons, which causes a net spin moment, for example, in Fe^{2+}, Fe^{3+}, Mn^{2+}. In the absence of an external field, the spins have random orientation and no net magnetization is observed. In an applied field the spins align statistically, which causes a magnetization parallel to the applied field, such that paramagnetic materials have a positive susceptibility. For an ion located in a crystal lattice, certain electron orbits are energetically preferred due to the

crystal field, that is, the charge distribution created by neighbouring atoms. Through spin–orbit coupling, the spins may show preferred orientation, which causes the paramagnetic anisotropy (O'Handley 2000). The paramagnetic response is stronger than the diamagnetic response, which is why diamagnetism is often neglected in materials with high Fe or Mn concentrations. Chemically pure alkali feldspar and plagioclase are solely diamagnetic. However, small amounts of Fe or Mn give rise to a dominant paramagnetic susceptibility.

This study focuses on the AMS of alkali feldspar and plagioclase single crystals, twins and crystals showing exsolution. We were particularly interested in (1) determining the intrinsic magnetic anisotropy due to the feldspar lattice and (2) examining whether ferromagnetic inclusions in feldspar have a systematic AMS with respect to the crystallographic axes. High-field methods were used in order to distinguish the diamagnetic/paramagnetic AMS associated with the silicate structure from any anisotropy due to ferromagnetic inclusions.

2 MATERIAL AND METHODS

2.1 Minerals of the feldspar group

The feldspar mineral group consists of two solid solution series. Members of the alkali feldspar solid solution series span the compositional range between K-feldspars (K[AlSi$_3$O$_8$]) and albite (Na[AlSi$_3$O$_8$]). Plagioclase forms a solid solution series with end-members albite and anorthite (Ca[Al$_2$Si$_2$O$_8$]). No significant solid solution exists between K- and Ca-feldspars, and there exists a miscibility gap between K-feldspar and albite that widens with decreasing temperature. Consequently, intermediate alkali feldspars often consist of an oriented intergrowth of K-feldspar and typically wormy or lamellar albite-rich feldspar that forms by exsolution upon slow cooling, and is referred to as perthite. Rarer antiperthite consists of alkali feldspar exsolutions in albite-rich feldspar. Other cations can be present in limited amounts; Fe^{3+} and Ti can replace Al; and Mg, Fe^{2+}, Sr and Mn can replace Ca. Clear yellow K-rich alkali feldspar from Madagascar can contain up to 10 per cent K[FeSi$_3$O$_8$] (Deer *et al.* 1992, 2001). Feldspars with elevated impurity element concentrations commonly form at high temperatures and may exsolve other minerals, such as oxides during slow cooling.

Feldspar is a tectosilicate consisting of a 3-D framework of corner-linked SiO$_4$ and AlO$_4$ tetrahedra. The larger, lower charge cations Na, Ca and K occupy cavities within this framework (Fig. 1). The overall topology is the same for all feldspars, but the detailed structure and crystal symmetry depend on composition, crystallization temperature and cooling history. Rapidly cooled high-temperature K-feldspar, sanidine, contains disordered Al and Si in the tetrahedral sites and retains monoclinic symmetry. Intermediate cooling rates can produce orthoclase, which exhibits monoclinic lattice symmetry, but Al and Si are partially or fully ordered on a local scale. Slowly cooled plutonic rocks and feldspars crystallized at low temperature tend to display ordered Al and Si, resulting in triclinic symmetry. This ordered K-rich feldspar is termed microcline. Albite and members of the plagioclase solid solution series are always triclinic, independent of Al/Si ordering. This is because Na and Ca are smaller cations than K, which causes distortions in the framework. These distortions are small, and all feldspars have identical framework topology and site distribution, so that they are expected to display similar dia/paramagnetic anisotropy.

Samples investigated in this study cover a range of compositions for alkali and plagioclase feldspars that represent the variety
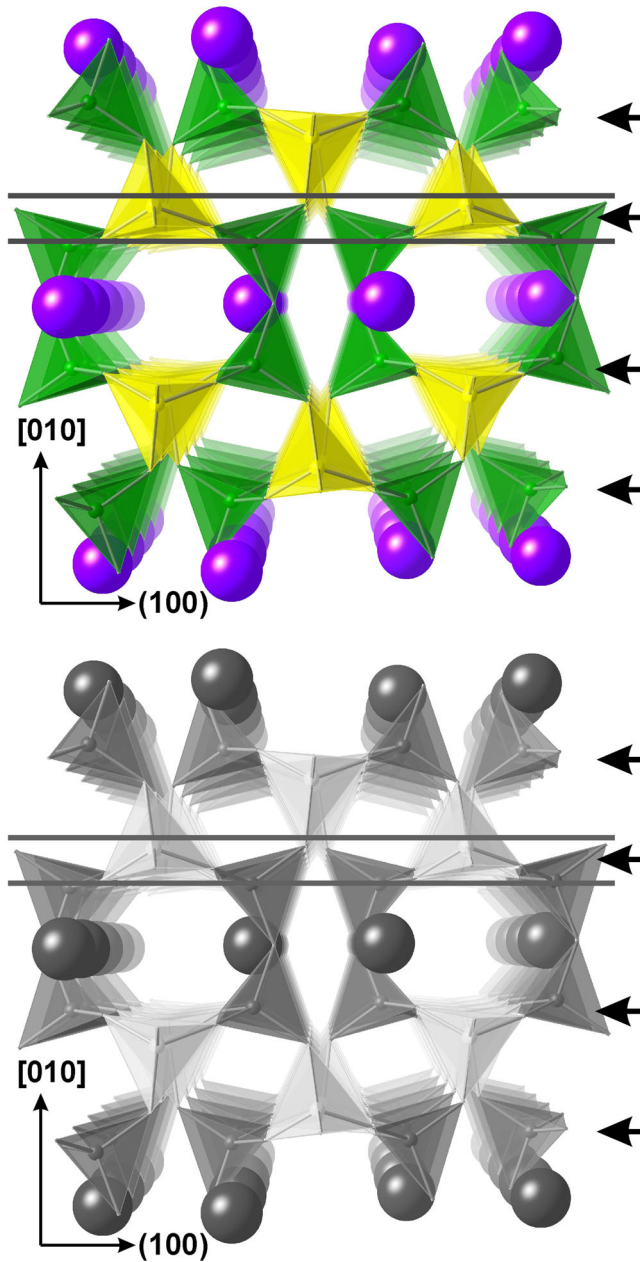
Figure 1. A perspective view of the tetrahedral framework of feldspar viewed down [001]. The positions of the large low-charge cations (K, Ca, Na) are represented as spheres. The majority of the oxygen atoms at the corners of the tetrahedra lie within planes parallel to (010) as indicated by the arrows and grey lines.

of structural states and compositions commonly found in nature. Feldspars are often twinned or multiply twinned in addition to perthitic and antiperthitic exsolution in alkali feldspars addressed above (Deer *et al.* 2001). Therefore, the sample suite included twinned and exsolved specimens as well as single crystals (Table 1). Twinning in triclinic feldspars, albite and perthite twinning, both result from the breaking of the monoclinic symmetry. Thus, twinned crystals will appear monoclinic. Given that the deviations from monoclinic symmetry in triclinic feldspars are small, and that twinning and exsolution preserves approximately the monoclinic symmetry, all specimens can be approximated as monoclinic for the purpose of this study.

2.2 Optical microscopy and crystal orientation

Optical microscopy was used to determine whether twinning or exsolution features were present within the crystals. Twinned samples were then oriented based on the known orientation of the twin lamellae, and single crystals based on their habit and Laue X-ray diffraction. Diffraction patterns were obtained at the Laboratory of Crystallography, ETH Zurich, and X-rays were generated in a Mo-tube operated at 35 mA and 50 kV. The sample was installed at *ca.* 40 mm distance from the image plate and Laue diffraction patterns were obtained in reflection mode with an exposure time of 4 min. Data analysis was performed using the OrientExpress 3.4 software (Laugier & Filhol 1983).

2.3 Chemical analysis

Elemental compositions of the crystals were determined using laser-ablation inductively coupled plasma mass spectroscopy (LA-ICP-MS) at the Institute of Geological Sciences, University of Bern. LA-ICP-MS was preferred over the more precise electron probe microanalysis because LA-ICP-MS integrates over a larger sample volume during analysis. Consequently, small-scale exsolution textures that form upon cooling of the crystal are analytically integrated to return the homogeneous high-temperature compositions of the feldspar crystals. Several spots were measured on each sample either on a crystal face, a polished crystal face, or a polished section. A detailed description of the experimental setup and parameters is given in Pettke *et al.* (2012). Measurements were performed with a beam diameter of 90 μm, and SRM610 was used as the external standard material. Data were processed using SILLS (Guillong *et al.* 2008). Mineral formulae were then recalculated in order to compute the orthoclase, albite and anorthite components for each sample.

2.4 Magnetic characterization and anisotropy of susceptibility

Magnetic measurements were performed at the Laboratory for Natural Magnetism, ETH Zurich. Acquisition of isothermal remanent magnetization (IRM) was measured on selected samples in order to characterize the type of ferromagnetic inclusions in the feldspar crystals. The samples were first magnetized in one direction in a 2 T-field and then progressively remagnetized in the opposite direction in increasing fields with an ASC-Scientific IM-10-30 pulse magnetizer. After each step, remanent magnetization was measured using a three-axis 2 G cryogenic magnetometer (Model 755). Hysteresis loops in fields up to 1 T were measured on a few samples using a Princeton Measurements Corporation MicroMag 3900 vibrating sample magnetometer (VSM), to further characterize the ferromagnetic inclusions.

Magnetic susceptibility is anisotropic and can be described by a second-order symmetric tensor. The three eigenvalues of this tensor are the principal susceptibilities, $k_1 \geq k_2 \geq k_3$, and the corresponding eigenvectors describe the directions of the principal susceptibility axes. For diamagnetic samples, we define k_1 as the most negative susceptibility and k_3 as the least negative susceptibility. Susceptibility can also be represented by a magnitude ellipsoid with semi-axes k_1, k_2 and k_3, whose shape is defined as (Jelinek 1981)

$$U = (2k_2 - k_1 - k_3)/(k_1 - k_3). \tag{1}$$

The shape parameter U can take on values between -1 and $+1$, where -1 corresponds to a rotationally prolate ellipsoid and $+1$

Table 1. Sample list and localities for the feldspar crystals. Samples are single crystals unless otherwise specified.

Sample	Mass (g)	Mineral	Locality	Comment
Alkali feldspar				
Am1	7.72	Amazonite	Colorado, US	
Am2	9.52	Amazonite	Colorado, US	
Am3	12.26	Amazonite	Colorado, US	
A1	2.7	Anorthoclase	Pili Mine, Chihuahua, Mexico	
Orth1	2.18	Orthoclase	Unknown	
Orth2	4.42	Orthoclase	Unknown	Carlsbad twin
Orth3	1.51	Orthoclase	Unknown	
Orth4	4.82	Orthoclase	Itrongay, Madagascar	
NMB127	5.99	Orthoclase	Goodsprings, Clark County, Nevada, US	
Fsp1	3.11	Orthoclase	China	
Kfsp1	0.65	Orthoclase	Massif Central, France	Carlsbad twin
NMB14622	3.48	Sanidine	Monte Amiata, Prov. Grosseto, Toscana, Italy	
Ad1	4.97	Adularia	Surselva, GR, Switzerland	
O1	6.77	Alkali feldspar	Unknown	Perthitic exsolution
O2	1.95	Alkali feldspar	Unknown	Perthitic exsolution
O3	7.91	Alkali feldspar	Unknown	Perthitic exsolution
O4	3.76	Alkali feldspar	Unknown	Perthitic exsolution
O5	6.08	Alkali feldspar	Unknown	Perthitic exsolution
O6	5.13	Alkali feldspar	Unknown	Perthitic exsolution
O7	6.92	Alkali feldspar	Unknown	Perthitic exsolution
Plagioclase				
Ab1	3.56	Albite (pericline)	Pfitsch, Tirol, Austria	Albite twin
NMB27181a	0.57	Andesine	Esterel, France	
NMB27181b	0.46	Andesine	Esterel, France	
Lab1	7	Labradorite	Madagascar	Polysynthetic twins
Lab2	6.2	Labradorite	Unknown	Polysynthetic twins
Lab3	7.5	Labradorite	Madagascar	Polysynthetic twins
Lab4	8.18	Labradorite	Madagascar	Polysynthetic twins
S1	7.78	Sunstone	Unknown	Platy inclusions
S2	8.35	Sunstone	Unknown	Platy inclusions
NMB45	2.11	Plagioclase	Fichtelgebirge, Bayern, Germany	
NMB28841	0.9	Plagioclase	Mt. Antero, Chaffe County, Colorado, US	

to a rotationally oblate ellipsoid. The degree of anisotropy can be described by

$$k' = \sqrt{\left[(k_1 - k_{\text{mean}})^2 + (k_2 - k_{\text{mean}})^2 + (k_3 - k_{\text{mean}})^2\right]/3}, \quad (2)$$

where

$$k_{\text{mean}} = \frac{1}{3}\,(k_1 + k_2 + k_3) \quad (3)$$

is the mean susceptibility (Jelinek 1984).

Low-field AMS provides information on the full susceptibility tensor from a superposition of diamagnetic, paramagnetic and ferromagnetic components. The low-field measurements were made on an AGICO MFK1-FA susceptibility bridge in magnetic fields of 200 or 500 A m^{-1} and a frequency of 976 Hz. Directional susceptibilities were measured using the stacking method outlined in Biedermann *et al.* (2013).

High-field AMS allows for separation of the magnetic anisotropy carried by the feldspar lattice from that carried by ferromagnetic inclusions. It was determined on a torque magnetometer in six fields between 1.0 and 1.5 T at room temperature and 77 K. The different field dependence of the diamagnetic and paramagnetic components as compared to the ferromagnetic component can be used to isolate each component provided that the magnetization of the ferromagnetic inclusions is saturated (Martín-Hernández & Hirt 2001). This is the case for inclusions of magnetite and maghemite. If hematite is also present, this component can be isolated using the method in Martín-Hernández & Hirt (2004). Schmidt *et al.*

(2007b) developed a method to isolate the diamagnetic from the paramagnetic component to the AMS, exploiting the temperature dependencies of the two magnetic fractions.

3 RESULTS

3.1 Twinning and exsolution features

About half of the samples display a clear diffraction pattern in combination with the typical feldspar habit, and are thus crystalline and homogeneous. Some specimens do not show clear diffraction patterns, even though their habit is characteristic for feldspar; this can be attributed to fine-scale twinning or exsolution processes. Alkali feldspar specimens O1–O7 did not show any diffraction pattern and show perthitic exsolution at various scales under the microscope (Fig. 2). Carlsbad twins were observed in Orth2 and Kfsp1. In plagioclase Lab2, one consistent set of twin lamellae is observed, suggesting simple polysynthetic twinning. Labradorites Lab1, Lab3 and Lab4 are aggregates of multiple grains. Sunstone samples S1 and S2 contain platy inclusions of opaque grains, which show a strong preferred orientation.

3.2 Chemical composition

A summary of the average elemental composition of each sample is given in Table A (Supporting Information) and recalculated formulae as well as concentrations of ions with strong magnetic
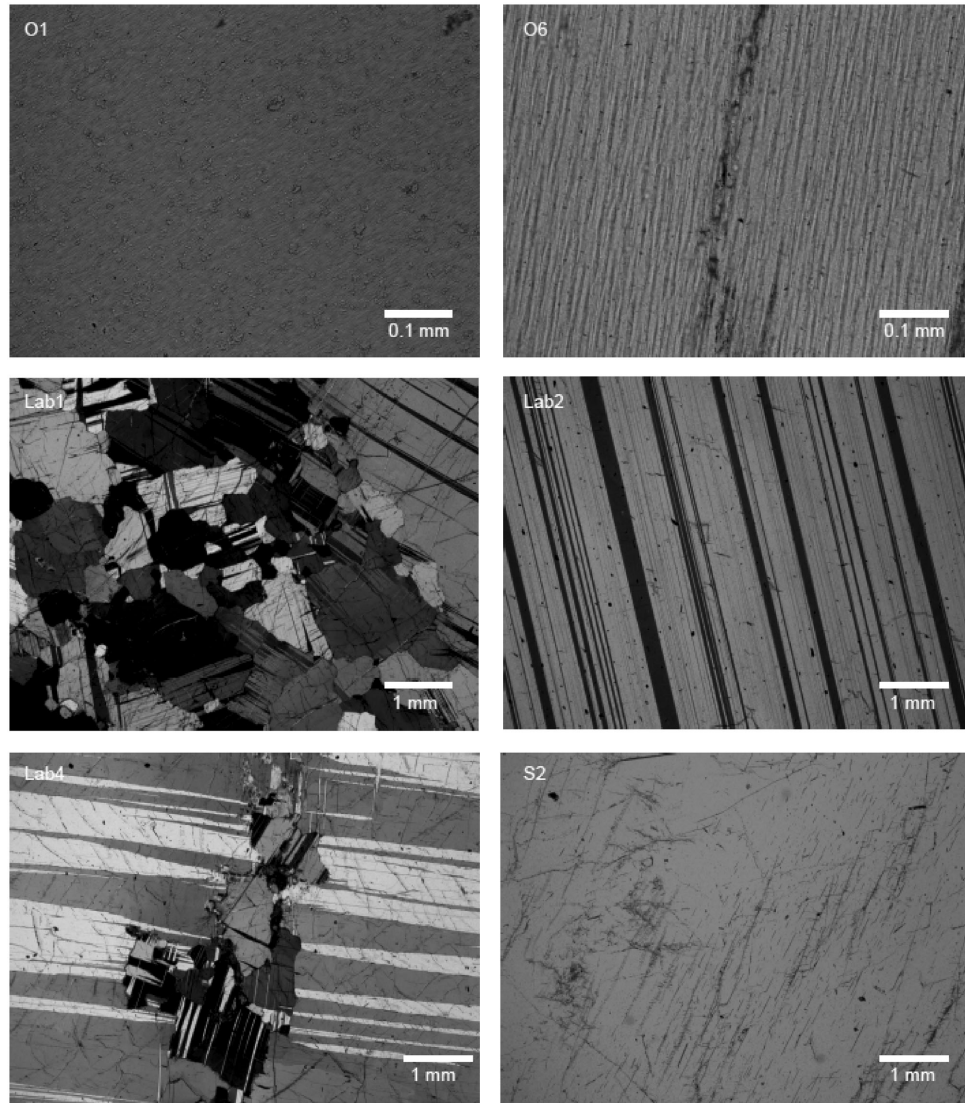
Figure 2. Thin section photographs of O1, O6, Lab1, Lab2, Lab4 and S2. The images of the labradorites were taken with crossed polarizers.

moment are shown in Table 2. Fig. 3 illustrates the broad range of compositions in the crystal collection, both in the alkali feldspar and plagioclase solid solution series. The distribution of the samples along the orthoclase (Or)–albite (Ab) and albite–anorthite (An) axes loosely traces the miscibility regions for feldspars, except for high-Ca end-members. Most specimens are compositionally homogeneous on the 100 μm scale as determined by LA-ICP-MS. Alkali feldspar samples Am1, Orth2 and Fsp1 reveal increased variability in Na_2O and K_2O along with constant Al_2O_3, indicating the presence of perthitic exsolution. For plagioclase, sample NMB27181a shows about 15 per cent variation in CaO along with increased variability of SiO_2 and Na_2O, suggesting prominent chemical zonation; samples NMB27181b, Lab3 and Lab4 show this too but less pronounced. Cations other than K, Na or Ca are present mostly in trace amounts. This also applies to the cations with strong magnetic moments, such as Fe, Mn and Ni, except for samples Orth3 (13300 μg g^{-1} Fe), A1 (5000 μg g^{-1} Fe) and Orth4 (3300 μg g^{-1} Fe). Crystal Orth3 contains the largest amount of iron, 0.07 atoms per formula unit, which is most likely present as Fe^{3+} replacing Al in the silicate framework. The Fe concentration in the other specimens varies between 5×10^{-5} and 0.02 atoms per formula unit. According to Smith & Brown (1988) hematite or copper plates are common in sunstone; however, neither Fe nor Cu show higher concentrations relative to other feldspar samples. In fact, none of the elements recorded in these sunstone samples show concentrations higher than for other feldspar samples (Table A).

3.3 Characterization of ferromagnetic inclusions

The ferromagnetic grains can be divided into two groups according to their magnetic behaviour (Fig. 4). In the first group, IRM increases rapidly in low fields, remanent coercivities are less than 50 mT and the magnetization approaches saturation by *ca.* 200 mT, whereas a weak increase can be observed in higher fields. This behaviour, shown by, for example, Orth2, Orth4, S1 and S2, suggests that two ferromagnetic phases are present, a low-coercivity phase, such as magnetite or maghemite, and a high-coercivity phase, such as hematite. Hysteresis loops measured on S1 and S2 are wasp-waisted, thus confirming the presence of both a low- and a high-coercivity phase (Fig. 5). In the second group, for example, Am1 or Orth1, the magnetization increases more slowly and does not reach saturation

Table 2. Recalculated cations per formula unit for main constituents and important magnetic ions based on LA-ICP-MS data.

Alkali feldspar

Sample	Am1	Am2	Am3	A1	Orth1*	Orth2	Orth3	Orth4	Fsp1	Kfsp1*	NMB14622	Ad1	O1	O2	O3	O4	O5	O6	O7
Si	2.99	2.96	2.95	2.99	2.88	2.94	3.04	2.99	2.97	2.97	2.97	2.94	2.96	2.97	2.95	2.95	2.95	2.94	2.96
Al	1.01	1.07	1.11	1.02	1.15	1.09	0.94	1.03	1.01	1.06	1.05	1.09	1.07	1.06	1.06	1.06	1.05	1.06	1.06
Ca	0.00	0.00	0.00	0.00	0.06	0.06	0.00	0.00	0.00	0.00	0.01	0.00	0.00	0.01	0.01	0.01	0.01	0.02	0.02
Na	0.08	0.17	0.07	0.58	0.04	0.18	0.01	0.05	0.07	0.34	0.16	0.02	0.26	0.27	0.27	0.30	0.31	0.32	0.29
K	0.92	0.77	0.82	0.39	0.88	0.67	1.01	0.90	1.03	0.62	0.76	0.97	0.70	0.64	0.73	0.69	0.70	0.68	0.67
Sum	5.00	4.97	4.94	4.98	5.00	4.93	5.00	4.97	5.08	4.99	4.96	5.01	4.99	4.95	5.02	5.02	5.02	5.03	4.99
Fe	0.00086	0.00097	0.00104	0.02438	0.00760	0.00388	0.06647	0.01662	0.00097	0.00552	0.00094	0.00005	0.00173	0.00133	0.00096	0.00192	0.00192	0.00302	0.00338
Mn	0.000010	0.000023	0.000006	0.000003	0.000405	0.000040	0.000027	<LOD	0.000002	0.000007	0.000004	<LOD	0.000003	0.000004	0.000004	0.000003	0.000003	0.000003	0.000031

Plagioclase

Sample	Ab1	NMB27181a	NMB27181b	Lab1	Lab2	Lab3	Lab4	S1	S2	NMB45	NMB28841
Si	2.94	2.62	2.60	2.53	2.55	2.55	2.55	2.72	2.73	2.59	3.34
Al	1.10	1.41	1.44	1.48	1.45	1.45	1.47	1.28	1.28	1.43	0.11
Ca	0.01	0.35	0.38	0.47	0.47	0.47	0.47	0.28	0.27	0.42	0.49
Na	0.93	0.58	0.51	0.45	0.45	0.45	0.45	0.68	0.70	0.51	1.33
K	0.01	0.01	0.01	0.03	0.04	0.03	0.03	0.01	0.01	0.01	0.00
Sum	4.98	4.97	4.94	4.97	4.96	4.96	4.96	4.98	4.98	4.96	5.27
Fe	0.00056	0.00514	0.00508	0.00538	0.00443	0.00352	0.00442	0.00204	0.00229	0.00386	0.00211
Mn	0.000029	0.000369	0.000298	0.000071	0.000105	0.000085	0.000078	0.000010	0.000009	0.000010	0.009101

*Marks samples for which the maximum CaO concentration was used for the calculation.
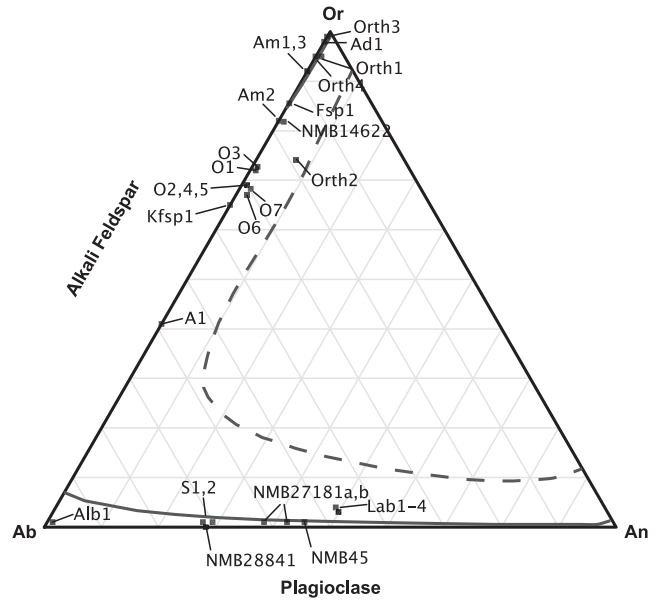

Figure 3. Ternary orthoclase (Or) – albite (Ab) – anorthite (An) diagram showing the chemical compositions of feldspars analysed. Crystals belonging to the Or–Ab series are termed alkali feldspar and those on Ab–An are plagioclase. Solid and dashed lines represent the miscibility gaps at 600 and 1000 °C (isotherms from Benisek *et al*. 2004).
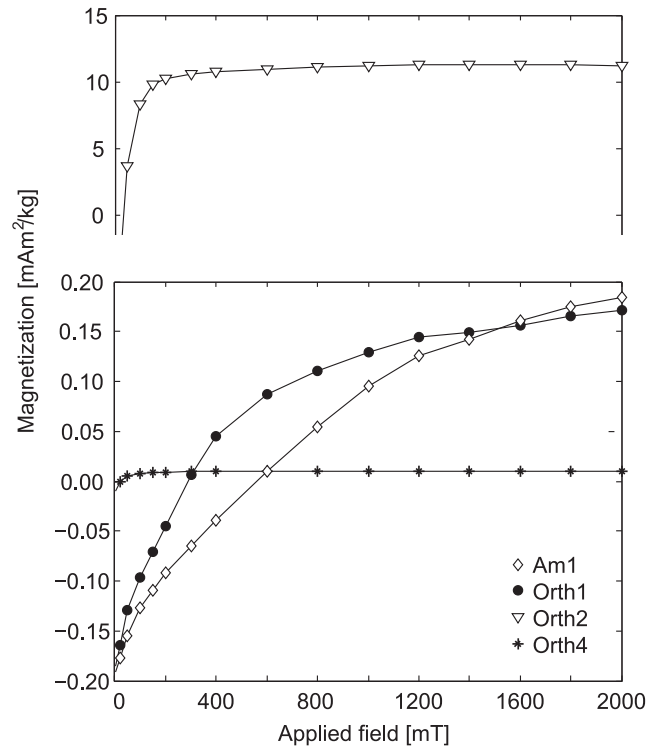

Figure 4. Representative IRM acquisition curves for selected feldspar crystals.

in fields up to 2 T. The remanent coercivities are between 300 and 600 mT (*cf*. Fig. 4). This suggests that the main ferromagnetic phase is hematite, although very small amounts of magnetite may also be present.
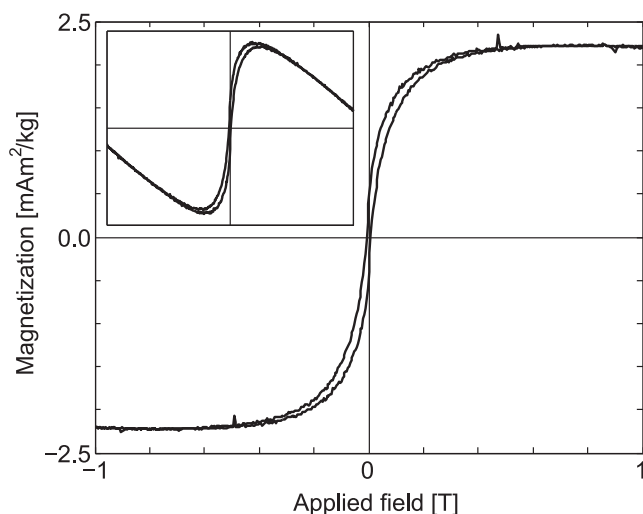
Figure 5. Hysteresis loop of sample S1, corrected for a linear diamagnetic contribution. Inset shows uncorrected hysteresis loop.

3.4 Magnetic susceptibility and anisotropy

The magnetic susceptibility of the feldspar samples is generally weak and ranges from -3.8×10^{-8} m^3 kg^{-1} to $+3.7 \times 10^{-7}$ m^3 kg^{-1} (Table B, Supporting Information). Seventeen specimens have negative mean susceptibilities and fourteen have positive ones. Because the mean susceptibility of many feldspar crystals is close to zero, the effect of a possible incomplete holder subtraction or magnetic susceptibility of the sample-holding glue can cause errors in the estimation of the mean susceptibility, particularly for small samples. Samples that appear weakly diamagnetic when measured on the MFK1-FA susceptibility bridge can have a small positive susceptibility when measured on a VSM, as has been observed for forsterite (Biedermann *et al.* 2014a).

Despite the weak mean susceptibility, a significant low-field AMS could be determined for all but three samples. One crystal, NMB27181b, displayed positive susceptibility in some directions and negative susceptibility in others, so that the AMS could not be determined. The directions of the principal axes of the susceptibility ellipsoid for the different crystals show no systematic relationship with the crystallographic axes (Fig. 6). Low-field anisotropy parameters are summarized in Table B.

Room-temperature high-field anisotropy is significant for all crystals except Ad1 and O4 (Table C, Supporting Information). The ferromagnetic contribution to the anisotropy is only significant in five alkali feldspars and three plagioclase samples. The sunstones S1 and S2 show similar principal ferromagnetic directions: their maximum ferromagnetic susceptibility is parallel to the elongation direction of the platy opaque inclusions. In the other samples, no systematic orientation of the principal ferromagnetic susceptibility axes to the feldspar lattice was observed.

The room-temperature high-field AMS is dominated by a diamagnetic or paramagnetic component, which amounts to >60 per cent of the torque signal. The degree of anisotropy k' varies from 2.60×10^{-11} m^3 kg^{-1} to 1.53×10^{-9} m^3 kg^{-1}. This range also includes Finkes (1909) result of $k' = 5.68 \times 10^{-10}$ m^3 kg^{-1}. The susceptibility becomes less anisotropic at 77 K compared to room temperature, or anisotropy is not significant at 77 K (Fig. 7).

Principal directions of the dia-/paramagnetic susceptibility at room temperature are shown in Fig. 6. For samples with positive mean susceptibility, the maximum susceptibility lies slightly canted to the crystallographic [001] axis and the minimum close to [010].

This applies to members of the alkali feldspar and plagioclase series; however, plagioclase shows slightly more scatter in direction than does alkali feldspar. The orientation of the principal axes can be explained by crystal symmetry, which requires that one principal susceptibility axis is parallel to [010] in monoclinic samples, whereas no symmetry constraints are imposed on triclinic crystals (Neumann 1885; Nye 1957). Some specimens that appeared to have negative susceptibilities exhibit similar principal directions as samples with positive mean susceptibilities. Because the torque magnetometer is sensitive to the magnitude of susceptibility differences within the measurement plane, but not to the direction of magnetization—parallel or antiparallel to the applied field — this may suggest that these crystals are also paramagnetic, if the same mechanism is responsible for the AMS as for the paramagnetic crystals. Amazonite (Am1-3) has a clear diamagnetic bulk susceptibility where its minimum (least negative) susceptibility is close to the [001] axis, whereas the maximum (most negative) susceptibility can be parallel to (100) or [010] depending on the sample.

4 DISCUSSION

Pure feldspar of ideal composition—independent of whether it is alkali feldspar or plagioclase—is diamagnetic. The susceptibility can become positive, however, (1) when cations with a strong magnetic moment, such as iron, enter the feldspar structure and/or (2) in the presence of ferromagnetic grains or other inclusions with strongly paramagnetic ions. According to Vernon (1961), a positive linear correlation is expected between iron concentration and mean susceptibility in ferromagnesian silicates. For feldspar, no such dependence on the mean susceptibility is observed either with Fe or Mn concentration or with a combination of the two weighted to their effective moments. Both negative and positive mean susceptibilities are measured for samples containing <2000 μg g^{-1} Fe. The three samples with higher iron concentration are all paramagnetic (Fig. 8). Large positive susceptibilities in the first group are attributed to ferromagnetic impurities, whereas Fe^{3+} may substitute for Al in Orth3 and Orth4, thus resulting in a paramagnetic susceptibility.

Magnetite/maghemite and hematite have been identified as ferromagnetic inclusions from the acquisition of IRM and hysteresis experiments, both in samples that carry a significant ferromagnetic anisotropy, and those that display none. In samples for which ferromagnetic anisotropy is observed, it does not have a consistent orientation with respect to the feldspar host, suggesting that these inclusions have no preferential orientation. For the two sunstone samples, the maximum ferromagnetic susceptibility is parallel to the long axes of the platy inclusions.

The magnetic anisotropy in the feldspar crystals is very weak. Although a significant anisotropy can be measured in low applied fields, there is no consistency in the orientation of the principal axes with respect to the crystallographic axes. The anisotropy which is determined in high fields at room temperature, however, shows a preferential grouping of the principal axes of the susceptibility ellipsoid. It is interesting to note that the high-field AMS measured at 77 K is not significant. Diamagnetic susceptibility is not dependent on temperature, whereas paramagnetic susceptibility varies inversely with temperature. Cooling the sample to 77 K will thus enhance the susceptibility of the paramagnetic ions. The fact that anisotropy is not significant at 77 K, therefore indicates that the observed susceptibility and anisotropy are superpositions of: (1) an isotropic paramagnetic component and (2) an anisotropic diamagnetic component. The paramagnetic component can be attributed
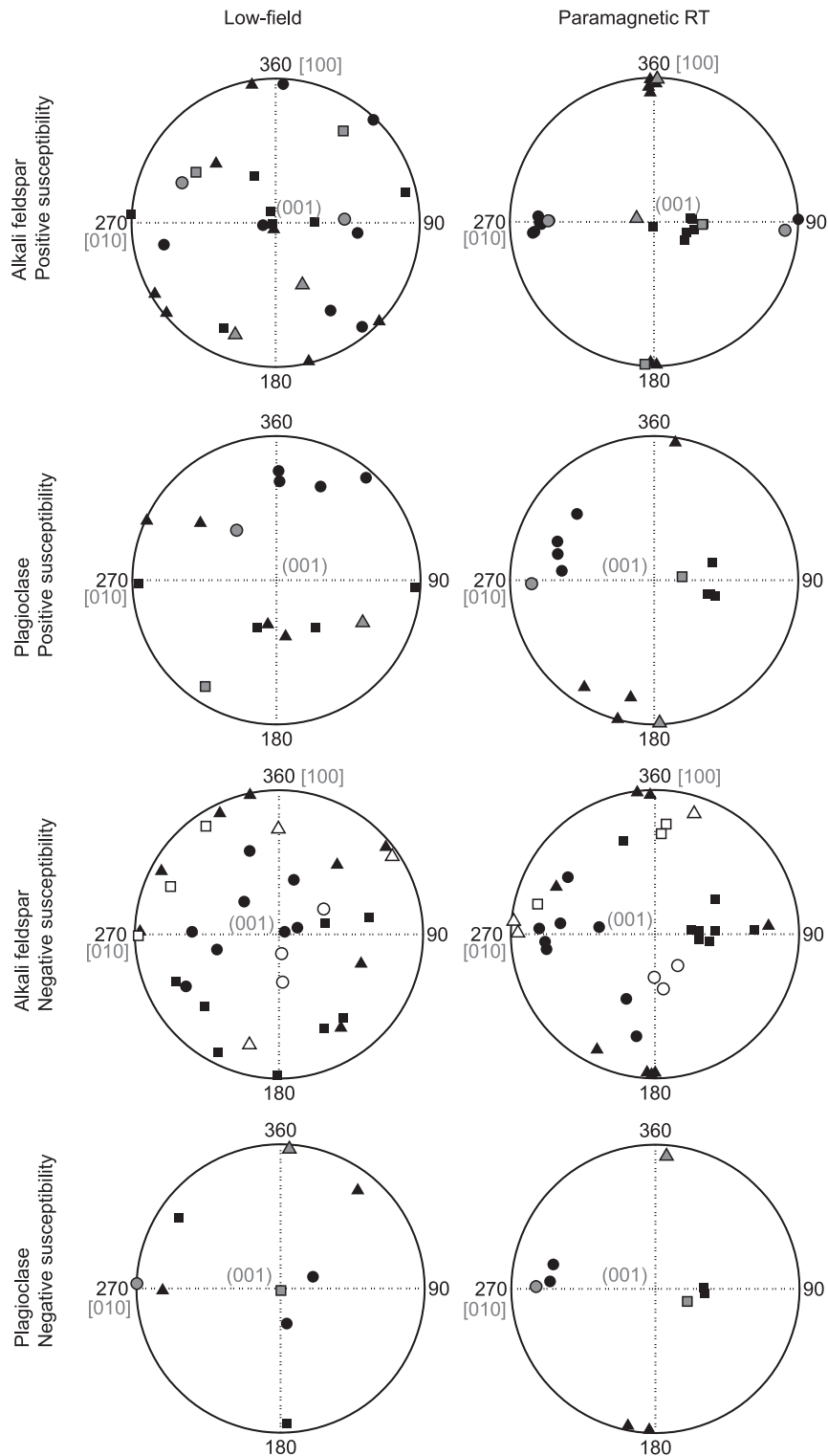
Figure 6. Equal-area lower hemisphere stereoplots showing principal low-field and dia/paramagnetic high-field susceptibility directions for alkali feldspar and plagioclase. Black symbols represent single crystals, grey symbols are twins and open circles represent amazonite. Squares, triangles and circles represent maximum, intermediated and minimum susceptibility, respectively.

to impurities, whereas the diamagnetic component is directly related to electron orbital contributions within the feldspar lattice. For the remainder of the text, we will refer to this component of the anisotropy as the diamagnetic AMS, regardless of whether the bulk susceptibility is positive or negative.

For samples with positive mean susceptibility, the k_1 axis lies close to the normal of the crystallographic (001) plane and k_3 is along [010] (Fig. 5). This agrees with observations by Selkin *et al.* (2000), who found the maximum susceptibility of an anorthosite to be close to the grouping of plagioclase [001] axes, and the minimum
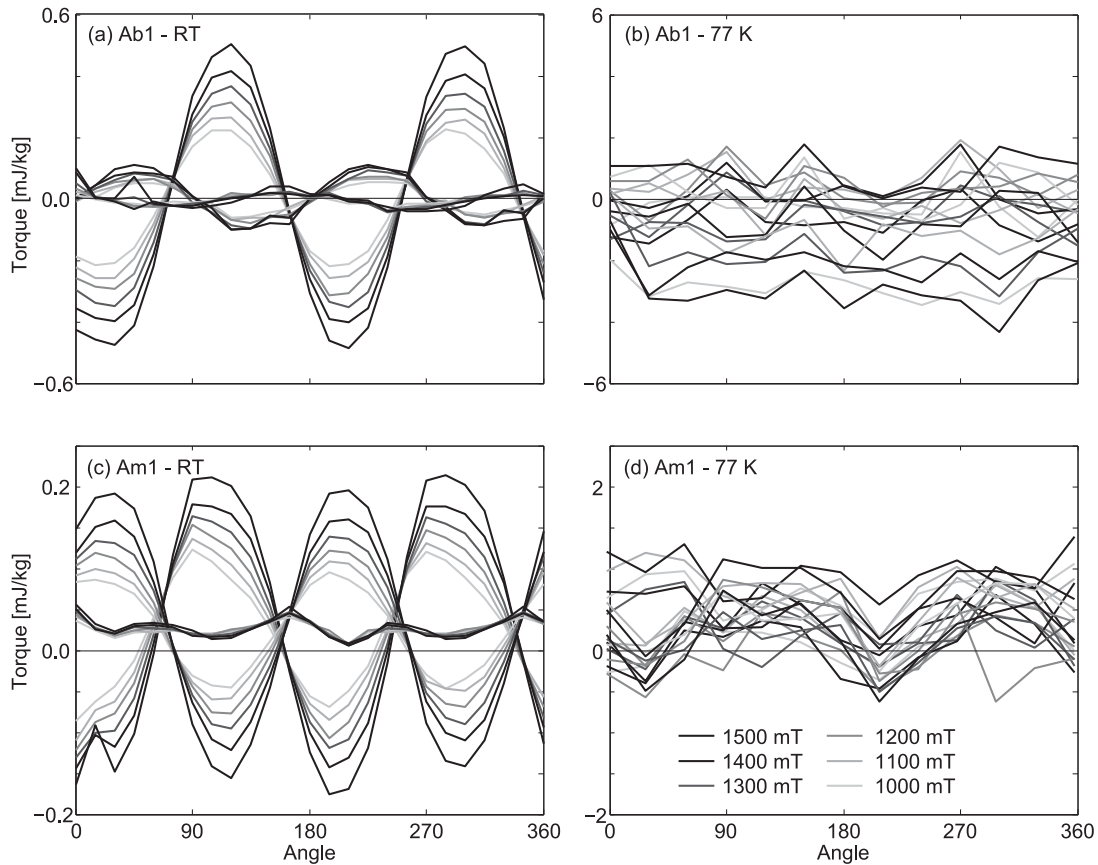
Figure 7. Torque signal at room temperature and 77 K for Ab1 and Am1. Torque as a function of angle is shown for three perpendicular planes and six applied fields.
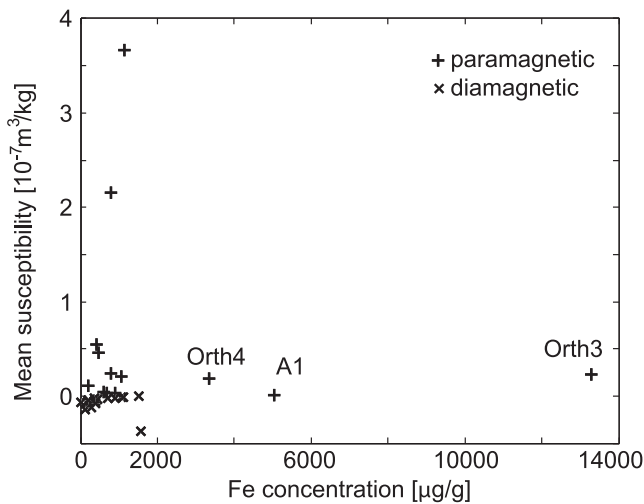

Figure 8. Mean susceptibility of feldspar as a function of Fe concentration.

susceptibility normal to foliation, that is, parallel to [010]. Based on the samples' bulk susceptibility, they suggested that the anisotropy arises from a ferromagnetic component due to inclusions in the feldspar. The discrepancy between the results reported in Selkin *et al.* (2014) and this study, is that we isolate the dia-/paramagnetic contribution to the AMS. Recall that diamagnetic anisotropy is related to differences in the size of the electron orbit when the field is applied in different directions. For example, the diamagnetic susceptibility in organic compounds or in graphite is largest normal to the plane in which the carbon rings are located (Krishnan 1934; Pauling 1936; McClure 1956). Similarly, the diamagnetic susceptibility in calcite and other carbonate minerals is largest parallel to the crystallographic [001] axis, which is normal to the planes in which the electron clouds are preferentially located (Pauling 1979a; Schmidt *et al.* 2007a). In feldspar, the majority of the bases of SiO_4 and AlO_4 tetrahedra are aligned quasi-parallel to the (010) planes (*cf.* Fig. 1). In an analogy to graphite or carbonates, the most negative susceptibility is therefore expected normal to the feldspar (010) planes, which can explain why the paramagnetic feldspars have their minimum susceptibility close to [010].

The ±[010] and ±[001] crystallographic axes have similar directions for the individuals in Carlsbad or albite twins and the principal susceptibility axes lie close to these directions. Therefore, the diamagnetic AMS is similar for the single crystals and the twinned crystals Orth2, Kfsp1, Ab1 and Lab2, that is, the maximum susceptibility is close to ±[001] and the minimum close to ±[010]. Deviations from this pattern only occur if the sample is not a pure single crystal or twin, but contains crystals with other orientations (e.g. intergrowths); in this case the orientations of the principal directions change. This effect is seen for samples Lab1, Lab3 and Lab4.

Amazonite is the only feldspar that deviates from this general relationship. All three amazonite samples have mean susceptibilities of -5×10^{-9} m^3 kg^{-1}, so that they are clearly diamagnetic and have their least negative susceptibility close to [001], whereas the diamagnetic adularia in Finkes (1909) study had its most negative susceptibility close to [001]. A possible explanation is the influence of H-containing defects in amazonite. The blue colour of these

specimens is related to Pb^{2+} and it appears that Pb^{2+} and OH^- defects in the feldspar structure are coupled (Smith & Brown 1988). It is known that water affects physical properties of minerals (e.g. Johnson 2006, and references therein). Similarly, H_2O or OH in the feldspar structure might affect magnetic properties by distorting the crystal lattice or changing the crystal field. For example, Koch-Müller *et al.* (2003) found that the unit cell of coesite, which has a framework similar to that of feldspar, changes when OH is incorporated. Interestingly, water occurs as OH in most feldspars but as H_2O in amazonite and microcline (Johnson 2006). The different size and charge of OH and H_2O could affect the distribution of the electrons and thus the diamagnetic AMS.

More work is clearly needed to fully explain the source of the diamagnetic, and possibly paramagnetic, AMS in feldspar. However, the dependence of principal susceptibility directions on the crystal structure established in this study can be used to interpret magnetic fabrics in anorthosites.

Compared to other rock-forming minerals, the mean susceptibility of feldspar is weak, and the same applies to its degree of anisotropy. The maximum degree of anisotropy of feldspar is 1.53×10^{-9} m^3 kg^{-1}. Typical AMS degrees for hornblende, augite or biotite are 9×10^{-9} m^3 kg^{-1}, 6×10^{-9} m^3 kg^{-1} and 4×10^{-8} m^3 kg^{-1} (Biedermann *et al.* 2014b, 2015a,b). Thus, the magnetic anisotropy of feldspar is a factor of 6 with respect to hornblende, 4 with respect to augite and 27 with respect to biotite weaker than the AMS of these mafic minerals that often occur together with feldspar in a rock. Even small amounts of preferentially aligned biotite (>4 per cent), augite (>20 per cent) or hornblende (>14 per cent) will dominate the magnetic anisotropy in a feldspar-dominated rock. A typical tonalite, for example, contains *ca.* 50 ± 10 per cent plagioclase and 10–20 per cent hornblende; gabbros generally contain 30–60 per cent plagioclase in addition to pyroxene, olivine and amphibole. Even though plagioclase dominates the modal composition in these rocks, its AMS is expected to be outweighed by that of the mafic minerals.

5 CONCLUSIONS

Feldspars possess a weak but significant magnetic anisotropy. Even though most samples have positive mean susceptibility, their AMS is dominated by a diamagnetic component related to preferred planes within the electron cloud, corresponding to a common plane of the bases of the Si- and Al-tetrahedra of the feldspar framework. The paramagnetic component is isotropic. The maximum susceptibility lies close to the crystallographic [001] axis and the minimum susceptibility is parallel to [010]. Feldspar often forms twins or exhibit exsolution features, and it is shown here that these samples show an AMS pattern similar to that of single crystals. This is not surprising given that the monoclinic symmetry is preserved by the twin laws. Consequently, AMS of feldspar can be used to infer the magnetic fabric in anorthosite. In other rocks, the feldspar fabric can play a role if they contain less than, for example, 4 per cent of biotite, 14 per cent of hornblende, or 20 per cent of augite with preferred orientation.

The ferromagnetic component of the AMS in feldspar only shows a consistent orientation of principal susceptibility axes in samples S1 and S2 that contain platy opaque grains. In these samples, the maximum ferromagnetic susceptibility is parallel to the elongation of the opaque grains, hence imaging their geometry. Most other samples did not show a significant ferromagnetic anisotropy. Thus, even though careful evaluation of the magnetic anisotropy is needed

for each rock, inclusions in feldspar should not in general be discarded as palaeofield recorders.

REFERENCES

Banerjee, S., 1939. The magnetic anisotropies of some organic crystals in relation to their structures, *Z. Kristallogr.*, **100,** 316–355.

Benisek, A., Kroll, H. & Cemic, L., 2004. New developments in two-feldspar thermometry, *Am. Mineral.*, **89,** 1496–1504.

Biedermann, A.R., Lowrie, W. & Hirt, A.M., 2013. A method for improving the measurement of low-field magnetic susceptibility anisotropy in weak samples, *J. appl. Geophys.*, **88,** 122–130.

Biedermann, A.R., Pettke, T., Reusser, E. & Hirt, A.M., 2014a. Anisotropy of magnetic susceptibility in natural olivine single crystals, *Geochem. Geophys. Geosyst.*, **15**(7), 3051–3065.

Biedermann, A.R., Bender Koch, C., Lorenz, W.E.A. & Hirt, A.M., 2014b. Low-temperature magnetic anisotropy in micas and chlorite, *Tectonophysics*, **629,** 63–74.

Biedermann, A.R., Pettke, T., Bender Koch, C. & Hirt, A.M., 2015a. Magnetic anisotropy in clinopyroxene and orthopyroxene single crystals, *J. geophys. Res.*, **120**(3), 1431–1451.

Biedermann, A.R., Bender Koch, C., Pettke, T. & Hirt, A.M., 2015b. Magnetic anisotropy in natural amphibole crystals, *Am. Mineral.*, **100,** 1940–1951.

Coe, R.S., 1979. The effect of shape anisotropy on TRM direction, *Geophys. J. R. astr. Soc.*, **56,** 369–383.

Cottrell, R.D. & Tarduno, J.A., 1999. Geomagnetic paleointensity derived from single plagioclase crystals, *Earth planet. Sci. Lett.*, **169,** 1–5.

Cottrell, R.D. & Tarduno, J.A., 2000. In search of high-fidelity geomagnetic paleointensities: a comparison of single plagioclase crystal and whole rock Thellier-Thellier analyses, *J. geophys. Res.*, **105**(B10), 23 579–23 594.

Davis, K.E., 1981. Magnetite rods in plagioclase as the primary carrier of stable NRM in ocean floor gabbros, *Earth planet. Sci. Lett.*, **55,** 190–198.

Deer, W.A., Howie, R.A. & Zussman, J., 1992. *An Introduction to the Rock-Forming Minerals*, 2nd edn, Longman Scientific and Technical, 696 pp.

Deer, W.A., Howie, R.A. & Zussman, J., 2001. *Framework Silicates: Feldspars*, 2nd edn, The Geological Society, 972 pp.

Evans, M.E. & McElhinny, M.W., 1966. The paleomagnetism of the Modipe Gabbro, *J. geophys. Res.*, **71**(24), 6053–6063.

Evans, M.E. & Wayman, M.L., 1974. An investigation of the role of ultra-fine titanomagnetite intergrowths in paleomagnetism, *Geophys. J. R. astr. Soc.*, **36,** 1–10.

Feinberg, J.M., Scott, G.R., Renne, P.R. & Wenk, H.-R., 2005. Exsolved magnetite inclusions in silicates: features determining their remanence behavior, *Geology*, **33**(6), 513–516.

Feinberg, J.M., Wenk, H.-R., Scott, G.R. & Renne, P.R., 2006. Preferred orientation and anisotropy of seismic and magnetic properties in gabbronorites from the Bushveld layered intrusion, *Tectonophysics*, **420**(3–4), 345–356.

Finke, W., 1909. Magnetische Messungen an Platinmetallen und monoklinen Kristallen, insbesondere der Eisen-, Kobalt- und Nickelsalze, *Ann. Phys.*, **336**(1), 149–68.

Fuller, M.D., 1960. Anisotropy of susceptibility and the natural remanent magnetization of some Welsh slates, *Nature*, **186**, 790–792.

Fuller, M.D., 1963. Magnetic anisotropy and paleomagnetism, *J. geophys. Res.*, **68**(1), 293–309.

Guillong, M., Meier, D.L., Allan, M.M., Heinrich, C.A. & Yardley, B.W.D., 2008. SILLS: a MATLAB-based program for the reduction of laser ablation ICP-MS data of homogeneous materials and inclusions, *Miner. Assoc. Canada Short Course*, **40**, 328–333.

Hargraves, R.B. & Young, W.M., 1969. Source of stable remanent magnetism in Lambertville diabase, *Am. J. Sci.*, **267**, 1161–1177.

Jelinek, V., 1981. Characterization of the magnetic fabric of rocks, *Tectonophysics*, **79**, T63–T67.

Jelinek, V., 1984. On a mixed quadratic invariant of the magnetic susceptibility tensor, *J. geophys.—Z. Geophys.*, **56**(1), 58–60.

Johnson, E.A., 2006. Water in nominally anhydrous crustal minerals: speciation, concentration, and geologic significance, *Rev. Mineral. Geochem.*, **62**, 117–154.

Koch-Müller, M., Dera, P., Fei, Y., Reno, B., Sobolev, N., Hauri, E. & Wysoczanski, R., 2003. OH$^-$ in synthetic and natural coesite, *Am. Mineral.*, **88**, 1436–1445.

Krishnan, K.S., 1934. Magnetic anisotropy of graphite, *Nature*, **133**(3353), 174–175.

Krishnan, K.S. & Ganguli, N., 1939. Temperature variation of the magnetic anisotropy of graphite, *Z. Kristallogr.*, **100**, 530–536.

Laugier, J. & Filhol, A., 1983. An interactive program for the interpretation and simulation of Laue patterns, *J. appl. Crystallogr.*, **16**, 281–283.

Martín-Hernández, F. & Hirt, A.M., 2001. Separation of ferrimagnetic and paramagnetic anisotropies using a high-field torsion magnetometer, *Tectonophysics*, **337**(3–4), 209–221.

Martín-Hernández, F. & Hirt, A.M., 2004. A method for the separation of paramagnetic, ferrimagnetic and haematite magnetic subfabrics using high-field torque magnetometry, *Geophys. J. Int.*, **157**(1), 117–127.

McClure, J.W., 1956. Diamagnetism of graphite, *Phys. Rev.*, **104**, 666–671.

Murthy, G.S., Evans, M.E. & Gough, D.I., 1971. Evidence of single-domain magnetite in the Michikamau anorthosite, *Can. J. Earth Sci.*, **8**, 361–370.

Neumann, F.E., 1885. *Vorlesungen über die Theorie der Elastizität der festen Körper und des Lichtäthers*, eds, Meyer, O.E. & Teubner, B.G., Verlag.

Nye, J.F., 1957. *Physical Properties of Crystals: Their Representation by Tensors and Matrices*, Clarendon Press, 322 pp.

O'Handley, R.C., 2000. *Modern Magnetic Materials: Principles and Applications*, 1st edn, Wiley.

Pauling, L., 1936. The diamagnetic anisotropy of aromatic molecules, *J. Chem. Phys.*, **4**, 673–677.

Pauling, L., 1979a. Diamagnetic anisotropy of the carbonate ion in calcite, aragonite, strontianite, and witherite and of other non-cyclic planar atomic groups with resonance structures, *Z. Kristallogr.*, **150**, 155–161.

Pauling, L., 1979b. Diamagnetic anisotropy of the peptide group, *Proc. Natl. Acad. Sci. USA*, **76**(5), 2293–2294.

Pettke, T., Oberli, F., Audétat, A., Guillong, M., Simon, A.C., Hanley, J.J. & Klemm, L.M., 2012. Recent developments in element concentration and isotope ratio analysis of individual fluid inclusions by laser ablation single and multiple collector ICP–MS, *Ore Geol. Rev.*, **44**, 10–38.

Schmidt, V., Günther, D. & Hirt, A.M., 2006. Magnetic anisotropy of calcite at room-temperature, *Tectonophysics*, **418**(1–2), 63–73.

Schmidt, V., Hirt, A.M., Hametner, K. & Gunther, D., 2007a. Magnetic anisotropy of carbonate minerals at room temperature and 77 K, *Am. Mineral.*, **92**(10), 1673–1684.

Schmidt, V., Hirt, A.M., Rosselli, P. & Martín-Hernández, F., 2007b. Separation of diamagnetic and paramagnetic anisotropy by high-field, low-temperature torque measurements, *Geophys. J. Int.*, **168**(1), 40–47.

Selkin, P.A., Gee, J.S., Tauxe, L., Meurer, W.P. & Newell, A.J., 2000. The effect of remanence anisotropy on paleointensity estimates: a case study from the Archean Stillwater Complex, *Earth planet. Sci. Lett.*, **183**, 403–416.

Selkin, P.A., Gee, J.S. & Meurer, W.P., 2014. Magnetic anisotropy as a tracer of crystal accummulation and transport, Middle Banded Series, Stillwater Complex, Montana, *Tectonophysics*, **629**, 123–137

Seront, B., Mainprice, D. & Christensen, N.I., 1993. A determination of the three-dimensional seismic properties of anorthosite: comparison between values calculated from the petrofabric and direct laboratory measurements, *J. geophys. Res.*, **98**(B2), 2209–2221.

Smith, J.V. & Brown, W.L., 1988. *Feldspar Minerals: Crystal Structures, Physical, Chemical and Microtextural Properties*, Springer.

Strangway, D.W., Larson, E.E. & Goldstein, M., 1968. A possible cause of high magnetic stability in volcanic rocks, *J. geophys. Res.*, **73**(12), 3787–3795.

Tarduno, J.A., Cottrell, R.D. & Smirnov, A.V., 2006. The paleomagnetism of single silicate crystals: recording geomagnetic field strength during mixed polarity intervals, superchrons, and inner core growth, *Rev. Geophys.*, **44**(1), RG1002, doi:10.1029/2005rg000189.

Uyeda, S., Fuller, M.D., Belshé, C. & Girdler, R.W., 1963. Anisotropy of magnetic susceptibility of rocks and minerals, *J. geophys. Res.*, **68**(1), 279–291.

Vernon, R.H., 1961. Magnetic susceptibility as a measure of total iron plus manganese in some ferromagnesian silicate minerals, *Am. Mineral.*, **46**, 1141–1153.

Wallace, P.R., 1947. The band theory of graphite, *Phys. Rev.*, **71**, 622–634.

Wenk, H.-R., Chen, K. & Smith, R., 2011. Morphology and microstructure of magnetite and ilmenite inclusions in plagioclase from Adirondack anorthositic gneiss, *Am. Mineral.*, **96**, 1316–1324.

Wu, Y.T., Fuller, M. & Schmidt, V.A., 1974. Microanalysis of NRM in a granodiorite intrusion, *Earth planet. Sci. Lett.*, **23**, 275–285.

SUPPORTING INFORMATION

Additional Supporting Information may be found in the online version of this paper:

Table A. Average elemental composition as defined by LA-ICP-MS.
Table B. Mean susceptibility and principal susceptibilities and directions of the low-field AMS with anisotropy degree, shape and significance. Directions are given when crystals could be oriented. Declination (D) and inclination (I) are given in a crystallographic coordinate system, where $D = 0$, $I = 0$ corresponds to [100], $D = 90$, $I = 0$ corresponds to [010] and $I = 90$ corresponds to (001) in monoclinic crystals and a direction normal to the plane defined by [100] and [010] for triclinic crystals.
Table C. Principal deviatoric susceptibilities and directions, AMS degree and shape of the (a) ferromagnetic component when significant and (b) diamagnetic/paramagnetic component of the AMS at room temperature and 77 K. Directions are given when crystals could be oriented and D and I are defined in the same way as for Table B.
(http://gji.oxfordjournals.org/lookup/suppl/doi:10.1093/gji/ggw042/-/DC1).

Please note: Oxford University Press is not responsible for the content or functionality of any supporting materials supplied by the authors. Any queries (other than missing material) should be directed to the corresponding author for the paper.